AIAA 81-1239R

Analysis of Stalled Airfoils by Simultaneous Perturbations to Viscous and Inviscid Equations

Bradford R. Gilmer* and Dean R. Bristow†
McDonnell Douglas Corporation, St. Louis, Mo.

An iterative viscous-inviscid interaction method is presented for predicting the pressures, forces, and moment of an arbitrary airfoil with massive turbulent separation in incompressible, steady flow. In each iteration cycle, the viscous-inviscid interaction is explicitly modeled by a mathematical expansion to a boundary-layer method and a panel method. Linear terms are retained to account for the complete first-order coupling between the viscous and inviscid equations. The system of linear, algebraic equations is solved for the perturbation to the displaced streamline geometry. Example calculations are presented that demonstrate consistently rapid convergence and good agreement with wind-tunnel data.

Nomenclature

C_D, C_L, C_M	= section drag, lift, and moment coefficient, respectively
C_P	= pressure coefficient, $= 1-(U/U_\infty)^2$
H	= boundary-layer shape factor
ISEP	= separation point index
ISTAG	= stagnation point index
ITR	= transition point index
i,j,k	= point on airfoil or streamline
n	= number of streamline defining points
n_B	= number of airfoil defining points
n_T	= number of unknowns
R_c	= chord Reynolds number
s	= surface distance
t	= fractional wake length
U	= velocity
α	= angle of attack
δ^*	= boundary-layer displacement thickness
θ	= angle with respect to x axis
Subscripts	
A,B	= first, last points in a flow region
B	= airfoil surface
D	= densely interpolated coordinates
LWR	= lower surface
SEP	= separation
T	= total
TE	= airfoil trailing edge
TR	= transition
UPR	= upper surface
WTE	= wake trailing edge
∞	= freestream conditions

Introduction

An iterative, coupled, viscous-inviscid interaction method has been developed for predicting the aerodynamic performance of single airfoils with massive turbulent separation in incompressible, steady flow. The objective of the method is to determine the effective inviscid (displaced) streamline and corresponding pressure distribution by applying a combination of surface singularity theory, boundary-layer theory, and a semiempirical separated wake model.

Although other iterative methods[1-4] have been developed for analyzing airfoils at high incidence, the present method is believed to be the first in which each iteration cycle is not divided into distinct viscous and inviscid calculation steps. Instead, both the viscous and inviscid equations are linearly expanded (or perturbed) about the solution from the preceding iteration cycle, and then the resulting system of coupled, linear equations is solved for the simultaneous prediction of the change in the viscous displacement thickness, pressure distribution, separation location, and wake length.

The motivation behind this fully coupled viscous-inviscid interaction approach is the quest for consistently reliable, rapid solution convergence without resorting to numerical smoothing or under-relaxation. In 1974 Brune et al.[5] successfully demonstrated a fully coupled approach for the special case of laminar, attached flow on a flat plate at zero angle of attack. The significance of the present method is that it handles arbitrary airfoil geometries with or without turbulent separation.

This paper presents the formulation of the method and comparison of example calculations with wind-tunnel data.

Formulation of the Method

The method is based on the hypothesis that there is an effective inviscid streamline for which the pressures calculated by inviscid theory will match the viscous pressures on the solid airfoil surface. The iterative solution approach requires representation of the effective inviscid streamline geometry by a finite array of unknowns. At the beginning of each iteration cycle, analytical derivatives are applied to establish first-order relationships between perturbations to the unknowns and the resulting perturbations to inviscid and viscous quantities. These first-order relationships are employed to develop a coupled viscous-inviscid system of linear, algebraic equations. The solution to these equations establishes a first-order correction to the array of unknowns.

The numerical formulation requires 1) a theoretical model for the conditions to be satisfied by the effective streamline, 2) a specialized, discrete geometric representation of the airfoil and streamline, 3) an inviscid panel method and a viscous boundary-layer method, and 4) a numerical procedure for coupling the viscous and inviscid methods. Each of these topics is discussed below.

Presented as Paper 81-1239 at the AIAA 14th Fluid and Plasma Dynamics Conference, Palo Alto, Calif., June 23-25, 1981; submitted June 14, 1981; revision received Feb. 12, 1982.

*Senior Engineer—Technology, Aerodynamics, McDonnell Aircraft Company. Member AIAA.

†Technical Specialist, Aerodynamics, McDonnell Aircraft Company. Member AIAA.

Displaced Streamline Theoretical Model

The effective inviscid streamline is represented by the theoretical model depicted in Fig. 1. Where the flow is attached, the streamline is the contour that is displaced from the airfoil surface by a distance equal to the boundary-layer displacement thickness δ^*. It is assumed that the location of boundary-layer transition from laminar to turbulent flow is known on the upper and lower surfaces. The location of turbulent separation is based on a critical value of the boundary-layer shape factor H. The streamline in the separation region is determined from the empirical observation that the pressure is constant between the separation point and the airfoil trailing edge. In the wake region, the streamline is established by a simple, zero-load, linear recovery of the velocity from the airfoil trailing edge value to approximately freestream conditions at the wake trailing edge.

Geometric Description

Two coordinate systems are employed (Fig. 2). The (x,y) Cartesian coordinate system is used for defining the surface of the solid airfoil and for the inviscid calculations to be made by a panel method. The (x',y') system is designated the boundary-layer coordinate system because x' measures distance along the solid surface and y' measures displacement normal to the surface.

A discrete set of input points $(x_B,y_B)_i$ is used to define the solid airfoil. The subscript i is ordered clockwise from the airfoil lower surface trailing edge ($i=1$) to the upper surface trailing edge ($i=n_B$). Typically, the number of points selected (n_B) is in the range 50-60. A conformal mapping routine[6] is used to interpolate on the array $(x_B,y_B)_i$, resulting in a much denser array $(x_D,y_D)_j$ where $1\leq j\leq 360$. The values $(x_D,y_D)_j$ remain invariant throughout all subsequent calculations for the airfoil.

The boundary-layer coordinate system (x',y') of Fig. 2 is used to define the displacement between the solid airfoil surface and the effective inviscid streamline. For arbitrary values of x' and y', a biquadratic curve fit routine and the enriched array $(x_D,y_D)_i$ are available in the present method for calculating the quantities x, $(\partial x/\partial x')$, $(\partial x/\partial y')$, and y, $(\partial y/\partial x')$, $(\partial y/\partial y')$. Four of these calculated quantities are coefficients in the following first-order relationships between geometric perturbations in the Cartesian coordinate system and the boundary-layer coordinate system:

$$dx=\left(\frac{\partial x}{\partial x'}\right)dx'+\left(\frac{\partial x}{\partial y'}\right)dy' \tag{1}$$

$$dy=\left(\frac{\partial y}{\partial x'}\right)dx'+\left(\frac{\partial y}{\partial y'}\right)dy' \tag{2}$$

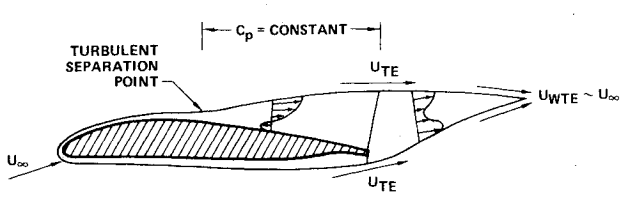

ATTACHED FLOW	AIRFOIL + δ^* →	CONVENTIONAL MODEL
SEPARATION POINT	PRESCRIBED H →	TURBULENT SEPARATION CONDITION
SEPARATED FLOW	C_p = CONSTANT →	SIMPLE SEPARATED FLOW MODEL
WAKE	LINEAR VELOCITY RECOVERY →	APPROPRIATE FOR SEPARATED OR FULLY ATTACHED FLOW

Fig. 1 Theoretical model for effective inviscid streamline.

The geometry of the effective inviscid streamline of an airfoil element is represented by a finite array of quantities (Fig. 3)

$x'_1\equiv 0$	y'_1	(lower trailing edge)
x'_2	y'_2	displacement from solid surface
↓	↓	
$x'_{n_B}\equiv s_B$	y'_{n_B}	(upper trailing edge)
Δs_{n_B}	θ_{n_B}	
Δs_{n_B+1}	θ_{n_B+1}	wake upper surface
↓	↓	
$\Delta s_{j_{WTE}-1}$	$\theta_{j_{WTE}-1}$	
$\Delta s_{j_{WTE}}$	$\theta_{j_{WTE}}$	
↓	↓	wake lower surface
Δs_{n-1}	θ_{n-1}	

where s_B is the perimeter of the solid airfoil, n_B the number of airfoil surface coordinates, $n-1$ the number of flat panels allocated for the streamline geometry representation, and j_{WTE} is the index of the wake trailing edge.

Before any aerodynamic calculations are performed, the following initial set of values is assigned to the effective inviscid streamline:

$$y'_1=y'_2=\ldots=y'_{n_B}=0 \tag{3}$$

$$\theta_{n_B}=\theta_{n_B+1}=\ldots=\theta_{j_{WTE}-1}=+\alpha \tag{4a}$$

$$\theta_{j_{WTE}}=\theta_{j_{WTE}+1}+\ldots=\theta_{n-1}=\pi+\alpha \tag{4b}$$

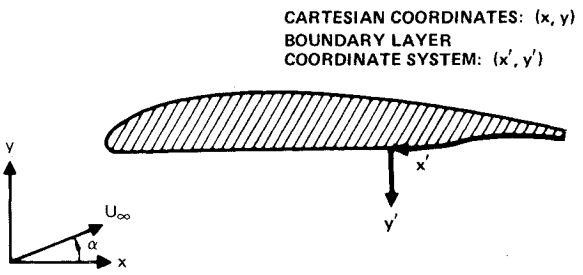

Fig. 2 Coordinate systems.

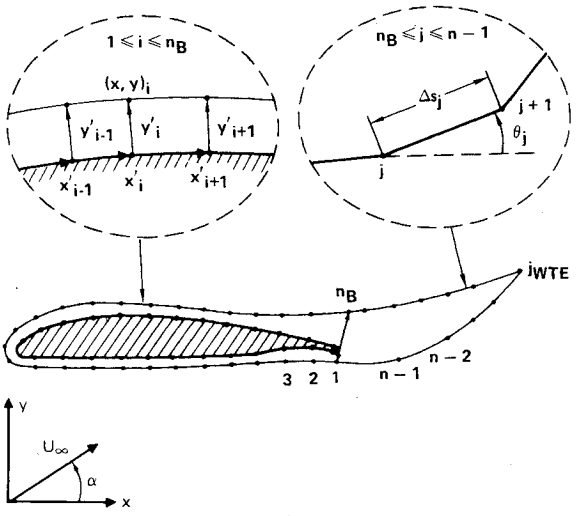

Fig. 3 Discretized representation of airfoil and streamline.

Table 1 Flow region index limits

Flow region	Index limits
Lower surface separated	$(1 \le i \le \text{ISEP}(1))$
Lower surface turbulent	$(\text{ISEP}(1) \le i \le \text{ITR}(1))$
Lower surface laminar	$(\text{ITR}(1) \le i \le \text{ISTAG})$
Upper surface laminar	$(\text{ISTAG} \le i \le \text{ITR}(2))$
Upper surface turbulent	$(\text{ITR}(2) \le i \le \text{ISEP}(2))$
Upper surface separated	$(\text{ISEP}(2) \le i \le n_B)$

This corresponds to the initial guess that the streamline is the solid airfoil surface with a straight trailing wake. The point indexing ($n_{B,j\text{WTE}}$, n) and the initial spacing ($x'_1,\ldots,x'_{nB}$; $\Delta s_{nB},\ldots,\Delta s_{n-1}$) are selected by the user.

The initial set of points (x'_1, $x'_2,\ldots,x'_{nB}$) is subdivided automatically (by a procedure to be described later) into one subset for each of the possible flow regions (Table 1).

At the angle of attack of interest, the region end point index limits of Table 1 do not change from one iteration cycle to the next. Thus, each panel continues to reside within the originally determined region. Furthermore, the relative spacing of points in a given flow region remains constant. This is expressed mathematically as

$$dx'_i = dx'_{i_A} + \frac{x'_i - x'_{i_A}}{s}\, ds \quad (i_A < i \le i_B) \tag{5}$$

where i_A and i_B are the index limits of the flow region of interest and where s is the region length ($s \equiv x'_{i_B} - x'_{i_A}$). Between successive iteration cycles, dx'_{i_A} and ds are usually nonzero. This corresponds to the fact that the endpoints of a region (e.g., stagnation or separation) are variables to be determined.

The upper and lower surface wake lengths are variables defined as

$$\text{WAKE UPR:} \quad s = \sum_{\text{UPR}} \Delta s_i \tag{6}$$

$$\text{WAKE LWR:} \quad s = \sum_{\text{LWR}} \Delta s_i \tag{7}$$

The fractional streamline surface distance from the airfoil trailing edge to panel endpoint i, designated t_i, is defined by Fig. 4. The relative spacing of points in the wake remain fixed during all the aerodynamic calculations at each angle of attack of interest. This is expressed mathematically as

$$dt_i = 0 \tag{8}$$

$$d(\Delta s_i) = (\Delta s_i / s)\, ds \tag{9}$$

The array of unknowns to be calculated that uniquely determines the effective inviscid streamline is designated the "g array," defined as

$$\begin{bmatrix} g_1 \\ g_2 \\ \downarrow \\ g_{n_T} \end{bmatrix} \equiv \begin{bmatrix} y'_1 \\ y'_2 \\ \downarrow \\ y'_{n_B} \\ \theta_{n_B} \\ \theta_{n_B+1} \\ \downarrow \\ \theta_{n-1} \\ s_{\text{LWR SEP}} \\ s_{\text{LWR TURB}} \\ \downarrow \\ s_{\text{UPR SEP}} \\ s_{\text{WAKE UPR}} \\ s_{\text{WAKE LWR}} \end{bmatrix} \tag{10}$$

If the flow on the upper and/or lower surface is fully attached, then $s_{\text{LWR SEP}}$ and/or $s_{\text{UPR SEP}}$ are exactly zero and are not included in the g array.

The following matrices, X_{ij}, Y_{ij}, X'_{ij}, and Y'_{ij}, are calculated at the beginning of each iteration cycle to determine the effect on geometry of first-order perturbations to the g array.

$$dx_i = \sum_j X_{ij}\, dg_j \tag{11a}$$

$$dy_i = \sum_j Y_{ij}\, dg_j \tag{11b}$$

$$dx'_i = \sum_j X'_{ij}\, dg_j \tag{11c}$$

$$dy'_i = \sum_j Y'_{ij}\, dg_j \tag{11d}$$

The calculation of the preceding matrices is based on analytical differentiation, a portion of which was performed in establishing Eqs. (1), (2), (5), and (9).

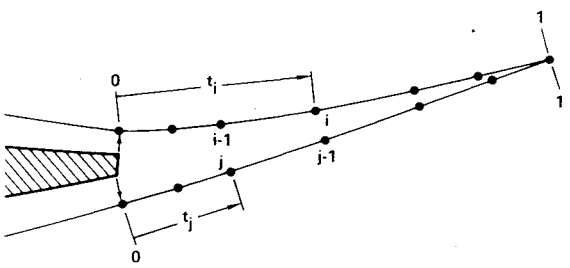

Fig. 4 Definition of fractional wake length parameter t.

Selected Numerical Methods

For inviscid analysis, the McDonnell Aircraft Company (MCAIR) two-dimensional panel method[7] is used to calculate the velocity and corresponding pressure coefficient at each panel midpoint and endpoint on the effective inviscid streamline. This method was chosen for its accuracy and insensitivity to panel spacing. Furthermore, the formulation for an inviscid perturbation matrix[7] was already available. The calculated inviscid velocity (U_i) at each endpoint i is the defining velocity distribution for the viscous analysis.

For viscous analysis, the Truckenbrodt integral boundary-layer method[8] is used to calculate the boundary-layer displacement thickness (δ_i^*), shape factor (H_i), and skin friction coefficient at each point x'_i in attached flow regions. The analysis starts at the stagnation location and proceeds streamwise to the airfoil trailing edge or to the separation location, if indicated. This method was chosen for its simplicity and relative insensitivity to point spacing.

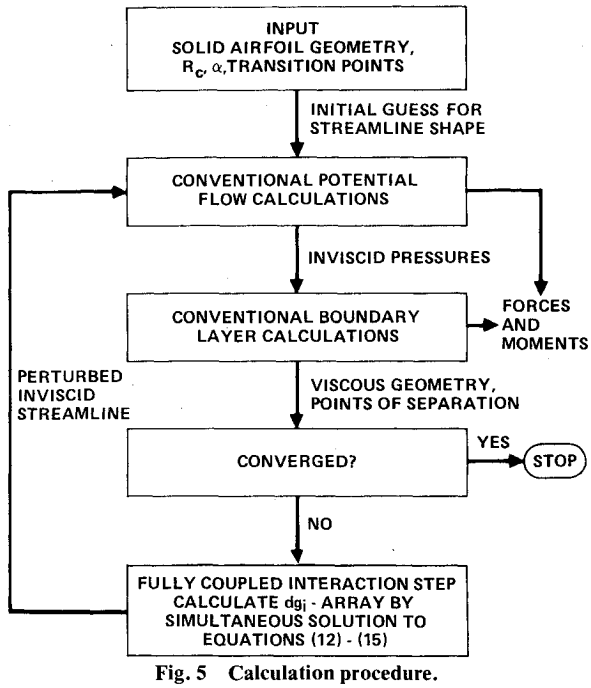

Fig. 5 Calculation procedure.

Calculation Procedure

The complete calculation procedure is illustrated schematically in Fig. 5. The first step is to define the airfoil geometry, freestream Reynolds number, angle of attack, and locations of boundary-layer transition from laminar to turbulent flow. The defined geometry is automatically converted to the enriched airfoil geometry $(x_D, y_D)_i$. The initial guess to the streamline geometry is based on the assumptions of Eqs. (3) and (4).

The next steps are to perform conventional inviscid and viscous analyses using the MCAIR panel method and Truckenbrodt boundary-layer method. After the analyses, the region limits of Table 1 are assigned. ISTAG is selected to be the index of the panel endpoint that is closest to the calculated stagnation location. Similarly, ITR(1) and ITR(2) are the indices of the panel endpoints closest to the prescribed transition locations on the lower and upper surfaces, respectively. ISEP(1) and ISEP(2) are, respectively, the indices of the most upstream lower and upper surface panel endpoints for which the boundary-layer shape factor H is greater than the critical separation value $H_{CRIT} = 3.2$. If there are no such points, the flow is assumed to be fully attached.

Next, a correction (perturbation) to the effective streamline geometry is to be determined. The perturbations to the g array (designated dg_i) are to be calculated such that all the modeling conditions depicted in Fig. 1 are simultaneously satisfied to first order

Region	Perturbation equation	
Attached flow	$\delta_i^* + d\delta_i^* = y_i' + dy_i'$	(12)
Separation location	$H_{i_{SEP}} + dH_{i_{SEP}} = H_{CRIT}$	(13)
Separated flow	$U_i + dU_i = U_{i_{SEP}} + dU_{i_{SEP}}$	(14)
Wake flow	$U_i + dU_i = U_{P_i} + dU_{P_i}$	(15)

where

$$U_{P_i} = U_{TE} + (U_{WTE} - U_{TE})t_i \quad (16)$$

$$dU_{P_i} = (1 - t_i)\,dU_{TE} \quad (17)$$

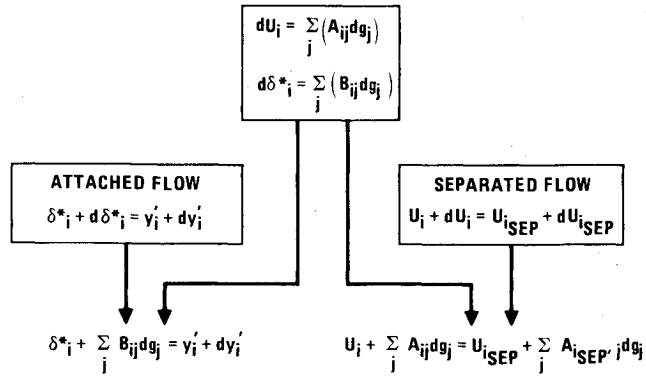

Fig. 6 Application of perturbation matrices to coupled viscous-inviscid interactions.

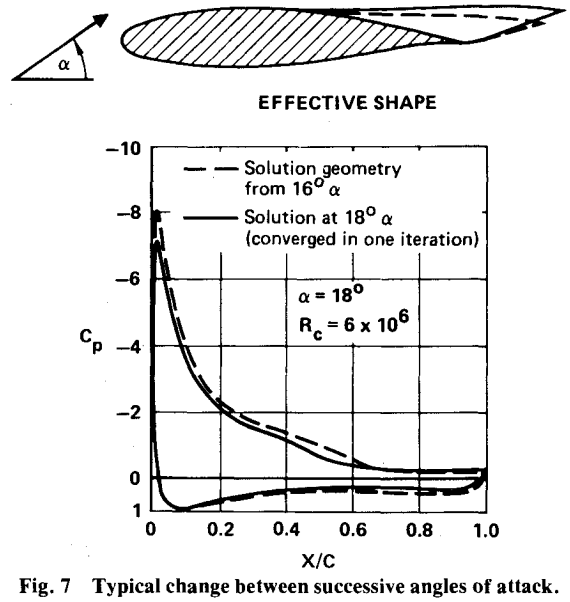

Fig. 7 Typical change between successive angles of attack.

In the preceding equations, i_{SEP} is ISEP(1) and/or ISEP(2), depending upon whether the airfoil lower and/or upper surface is separated. The airfoil trailing-edge velocity U_{TE} designates either U_l or U_{nB}, which are to be equal. The wake trailing-edge velocity U_{WTE}, which is slightly less than freestream velocity U_∞, is selected by the user.

Equation (12) corresponds to the condition that the updated (perturbed) streamline displacement and boundary-layer displacement thickness are to be equal. The panel endpoint selected to be the separation point is to move such that the updated shape factor $(H_{i_{SEP}} + dH_{i_{SEP}})$ will be the prescribed separation value [Eq. (13)]. As a direct consequence of Bernoulli's law, the separated flow model of constant pressure is equivalent to Eq. (14), i.e., the updated velocity in the separated region is to equal the velocity at the updated separation point. The linear wake velocity recovery model is expressed by Eq. (15); the updated prescribed velocity $(U_{P_i} + dU_{P_i})$ varies linearly with distance from the airfoil trailing edge to approximately freestream velocity at the wake trailing edge.

In order to determine the set of values dg_i $(1 \le i \le n_T)$ that satisfies Eqs. (12-15), it is first necessary to relate the aerodynamic perturbation quantities $d\delta_i^*$, dH_i, and dU_i to the unknowns dg_i. As discussed in the Appendix, perturbation matrices A_{ij}, B_{ij}, and C_{ij} are calculated such that

$$dU_i = \sum_j A_{ij} dg_j + 0(dg^2) \quad (18)$$

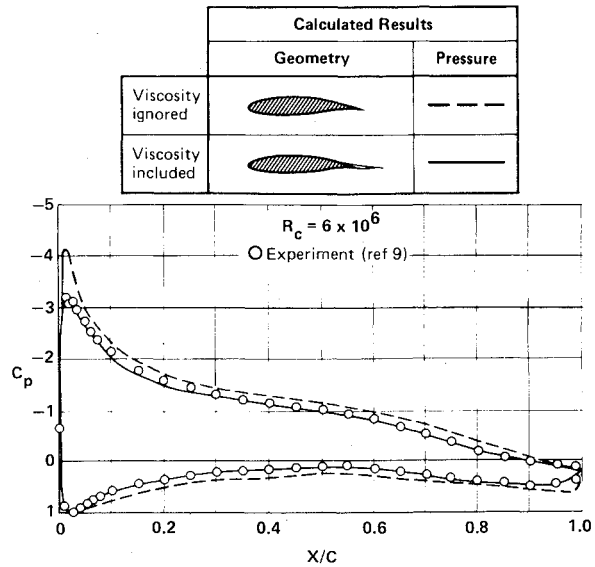

Fig. 8 Prediction accuracy at low angle of attack (8 deg), NASA GA(W)-1.

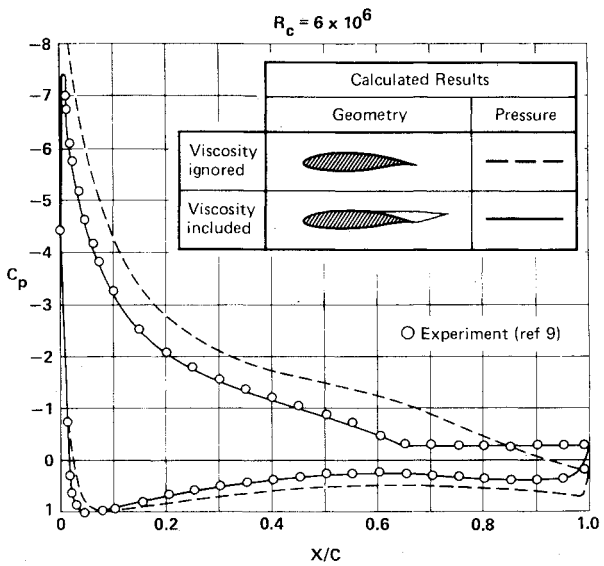

Fig. 9 Prediction accuracy at high angle of attack (16 deg), NASA GA(W)-1.

$$d\delta_i^* = \sum_j B_{ij} dg_j + 0(dg^2) \tag{19}$$

$$dH_i = \sum_j C_{ij} dg_j + 0(dg^2) \tag{20}$$

As illustrated in Fig. 6, the substitution of Eqs. (18-20) into Eqs. (12-15) establishes a system of linear, algebraic equations in terms of the unknowns dg_j. The perturbation equations include the simultaneous coupling of viscous and inviscid theories. However, the equations are not complete. It is necessary to introduce seven additional equations corresponding to the constraints that 1) point ISTAG is to be the stagnation point, 2) points ITR(1) and ITR(2) are to match the prescribed transition locations, 3) x_1' and x_{nB}' are to be zero and s_B, respectively, and 4) the inviscid streamline is to be continuous (points 1 and n are to coincide). These additional constraint equations are discussed in the Appendix. Furthermore, the separated flow and wake flow endpoint velocity perturbation equations, Eqs. (14) and (15), are numerically unstable.[7] It is necessary to introduce additional perturbation equations, identical to Eqs. (14) and (15), for the velocity at panel midpoints in the separated and wake regions.

The total number of linear, algebraic, perturbation equations exceeds the number of unknowns. Consequently, the solution for the values dg_j is accomplished by using the method of least square errors. A very high weighting based on local point spacing is applied to the satisfaction of Eq. (12). Equation (13) and the constraint equations of the Appendix are satisfied exactly by using Lagrangian multipliers. A reduced weighting based on local panel dimensions in the separated and wake regions is applied to the satisfaction of Eqs. (14) and (15) for both panel endpoints and midpoints. With the aid of standard matrix methods, the solution array dg_i $(1 \le i \le n_T)$ is calculated.

The final steps in the calculation procedure are to update the g array by adding the calculated dg_i and to apply the updated g array to the construction of a corrected streamline geometry. A test is made to verify that the streamline is nearly continuous at points 1 and n and that U_{iSTAG} is approximately equal to zero. If either condition is not met, appropriate modifications are made automatically. The calculation sequence is then returned to the inviscid calculation step.

This iterative procedure is continued until convergence to a prescribed tolerance is obtained. Forces and moment are calculated by integrating the calculated pressure at each panel midpoint and the skin friction at each panel endpoint over the solid airfoil surface.

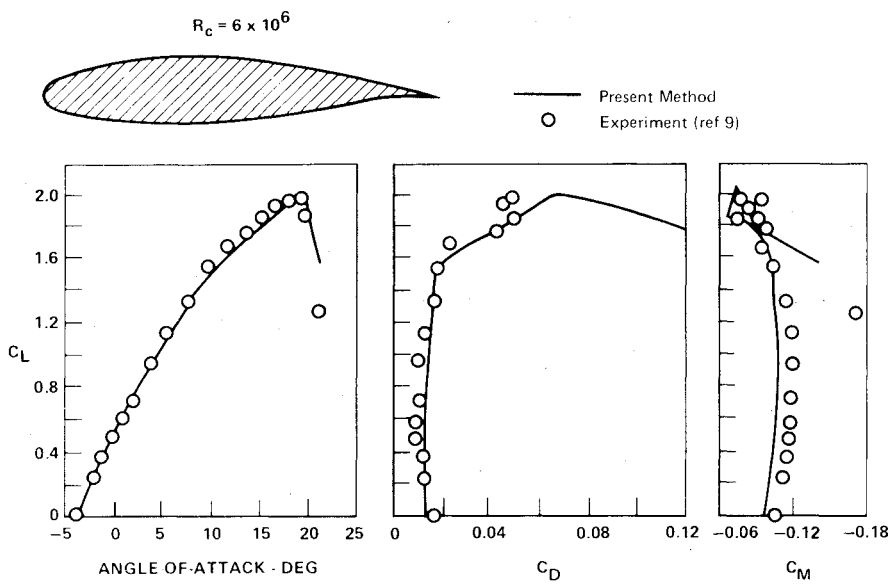

Fig. 10 Accuracy of force and moment predictions, NASA GA(W)-1.

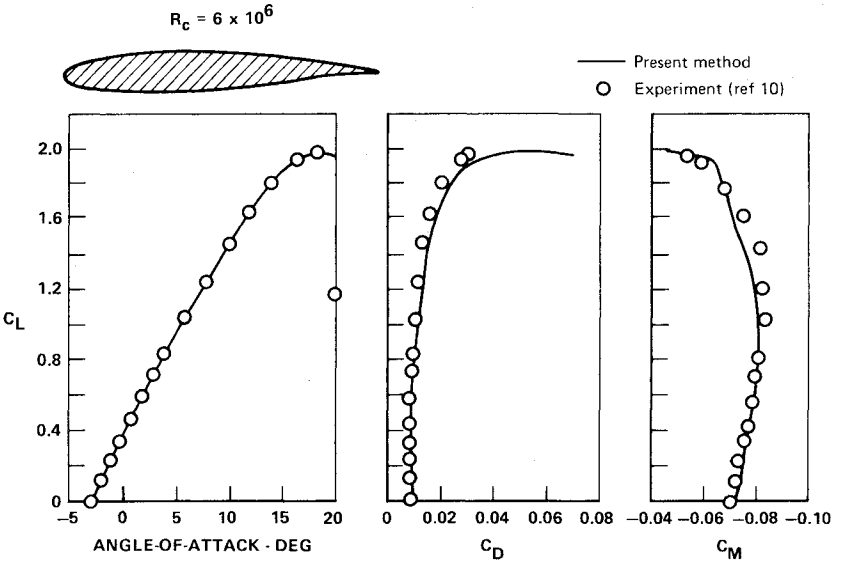

Fig. 11 Accuracy of force and moment predictions, NASA MS(1)-0313.

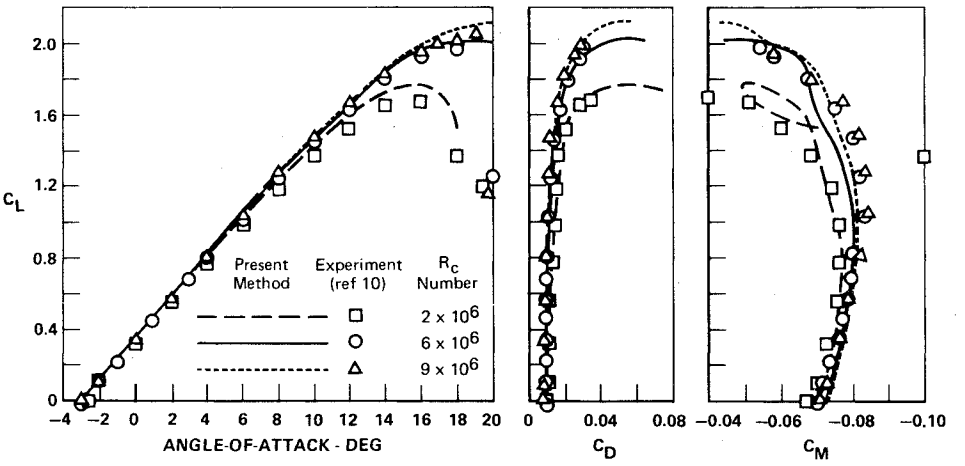

Fig. 12 Effect of Reynolds number on force and moment, NASA MS(1)-0313.

In the present method the calculation of lift, drag, and moment with respect to angle of attack is usually performed in two degree increments. The converged solution geometry at each angle of attack then provides the starting (or initial guess) geometry for the subsequent angle of attack. Because all of the viscous and inviscid interactions are included simultaneously, one to three iteration cycles are usually sufficient for each additional angle of attack (Fig. 7).

Example Calculations

The present method was used to calculate the forces and moment on three different airfoils that exhibit trailing-edge separation. Figures 8 and 9 show calculated and experimental[9] pressure distributions for typical attached and separated flow cases. It is apparent that the effect of viscosity is significant even for attached flow, and that the present method accurately predicts the effect. Lift, drag, and moment predictions vs angle of attack are compared with experiments in Figs. 10 and 11 for the GA(W)-1 and MS(1)-0313 airfoils.[9,10] The effect of Reynolds number on forces and moment for the MS(1)-0313 is depicted in Fig. 12. The agreement with experimental data is good in all cases. Similar results were obtained for the MS(1)-0317 airfoil; however, the test data are restricted and cannot be presented here.

For the example calculations, the number of streamline panels employed for the different airfoils were 72 for the GA(W)-1 and 66 for the MS(1)-0313. No special consideration was given to the panel spacing. Numerical studies indicate that very dense paneling does not appreciably alter the accuracy or convergence of the present method.

Conclusions

Experience with the present method for both attached and separated flow cases has resulted in the following conclusions.

1) Predictions agree well with test data.

2) Convergence is rapid and reliable.

3) 65-75 panels are adequate for modeling the effective streamline.

4) Prediction accuracy is insensitive to panel spacing.

5) No numerical smoothing is required.

6) The computing time is typically 25-30 CP seconds per iteration on the MDC CYBER 750 computer.

Appendix

The section entitled Calculation Procedure requires 1) an inviscid perturbation matrix that relates the change in the streamline surface velocity to geometric perturbations, 2) viscous perturbation matrices that relate the change in the boundary-layer displacement thickness and shape factor to geometric perturbations, and 3) constraint equations that control the location of each of the flow region endpoints. The procedure for establishing these relationships is summarized next.

Inviscid Expansions

The inviscid velocity geometry perturbation matrix A_{ij} is determined by analytically expanding the MCAIR panel method. The panel method determines the velocity at the endpoint of each panel i (U_i) from the freestream conditions and the geometry of influencing panels, $(x,y)_j$, $1 \le j \le n-1$.

This can be stated functionally as

$$U_i = f_1(U_\infty, \alpha, x_j, y_j) \tag{A1}$$

Noting that the freestream conditions do not change during perturbation and that coordinates x_j and y_j can be related to the g array [Eq. (11)], the first-order expansion to Eq. (A1) becomes

$$dU_i = \sum_j \frac{\partial f_1}{\partial g_j} dg_j \equiv \sum_j A_{ij} dg_j \tag{A2}$$

The procedure for calculating A_{ij} is to repeat each step in the panel method formulation, replacing each mathematical quantity by its differential with respect to geometric perturbation. A more detailed discussion of this procedure is available in Ref. 7.

Viscous Expansions

The viscous perturbation matrices B_{ij} and C_{ij} are determined by analytically expanding the numerical formulation of the Truckenbrodt boundary-layer procedure. The boundary-layer method relates the displacement thickness δ^* and shape factor H at each point x_i' to the upstream history. This can be stated functionally as

$$\delta_i^* = f_2(R_c, \delta_{i-1}^*, H_{i-1}, x_{i-1}', U_{i-1}, x_i', U_i) \tag{A3}$$

$$H_i = f_3(R_c, \delta_{i-1}^*, H_{i-1}, x_{i-1}', U_{i-1}, x_i', U_i) \tag{A4}$$

For fixed Reynolds number R_c, a first-order expansion to Eq. (A3) is

$$d\delta^* = \frac{\partial f_2}{\partial \delta_{i-1}^*} d\delta_{i-1}^* + \frac{\partial f_2}{\partial H_{i-1}} dH_{i-1} + \frac{\partial f_2}{\partial x_{i-1}'} dx_{i-1}' + \frac{\partial f_2}{\partial U_{i-1}} dU_{i-1} + \frac{\partial f_2}{\partial x_i'} dx_i' + \frac{\partial f_2}{\partial U_i} dU_i \tag{A5}$$

The B and C matrices for $d\delta^*$ and dH are presumed to be known at the upstream station $i-1$. The inviscid expansions establish the A matrix for dU for all panels. The dx' terms are related to dg_k by Eq. (11). Thus, Eq. (A5) becomes

$$d\delta_i^* = \frac{\partial f_2}{\partial \delta_{i-1}^*} \sum_j B_{i-1,j} dg_j + \frac{\partial f_2}{\partial H_{i-1}} \sum_j C_{i-1,j} dg_j + \frac{\partial f_2}{\partial x_{i-1}'} \sum_j X_{i-1,j}' dg_j + \frac{\partial f_2}{\partial U_{i-1}} \sum_j A_{i-1,j} dg_j + \frac{\partial f_2}{\partial x_i'} \sum_j X_{ij}' dg_j + \frac{\partial f_2}{\partial U_i} \sum_j A_{ij} dg_j \tag{A6}$$

Equation (A6) reduces to

$$d\delta_i^* = \sum_j B_{ij} dg_j \tag{A7}$$

Similarly for dH, Eq. (A4) becomes

$$dH_i = \sum_j C_{ij} dg_j \tag{A8}$$

where B_{ij} and C_{ij} are matrices that are calculated as explicit functions of array dg.

Constraint Equations

There is one or more constraint equation for each region endpoint. Two constraints keep the airfoil lower and upper trailing edges fixed

$$x_1' + dx_1' = 0 \tag{A9}$$

$$x_{n_B}' + dx_{n_B}' = s_B \tag{A10}$$

The lower and upper locations of transition are required to be the prescribed input values ($x_{\text{TR LWR}}'$ and $x_{\text{TR UPR}}'$)

$$x_{\text{ITR}(1)}' + dx_{\text{ITR}(1)}' = x_{\text{TR LWR}}' \tag{A11}$$

$$x_{\text{ITR}(2)}' + dx_{\text{ITR}(2)}' = x_{\text{TR UPR}}' \tag{A12}$$

The chosen stagnation panel endpoint is required to have a velocity of magnitude zero

$$U_{i_{\text{STAG}}} + dU_{i_{\text{STAG}}} = 0 \tag{A13}$$

The value of the shape factor at the lower and/or upper turbulent separation point is required to be the input value [equivalent to Eq. (13)]

$$H_{i_{\text{SEP}(1)}} + dH_{i_{\text{SEP}(1)}} = H_{\text{CRIT}} \tag{A14}$$

$$H_{i_{\text{SEP}(2)}} + dH_{i_{\text{SEP}(2)}} = H_{\text{CRIT}} \tag{A15}$$

The wake geometry must close

$$x_1 + dx_1 = x_n + dx_n \tag{A16}$$

$$y_1 + dy_1 = y_n + dy_n \tag{A17}$$

All of the preceding constraint equations are linearized with respect to dg_j.

Acknowledgments

This work was supported by the McDonnell Aircraft Company 1980 Independent Research and Development Program.

References

[1] Maskew, B. and Dvorak, F. A., "Investigation of Separation Models for the Prediction of $C_{L_{\max}}$," *Journal of the American Helicopter Society*, Vol. 23, April 1978, pp. 2-8.

[2] Henderson, M. L., "A Solution to the 2-D Separated Wake Modeling Problem and Its Use to Predict $C_{L_{\max}}$ of Arbitrary Airfoil Sections," AIAA Paper 78-156, Jan. 1978.

[3] Le Balleur, J. C. and Néron, M., "Calcul D'Ecoulements Visqueux Decolles sur Profils D'Ailes par une Approche de Couplage," *AGARD Conference Proceedings*, No. 291, Feb. 1981, pp. 11-1 to 11-5.

[4] Carlson, L. A., "A Direct-Inverse Technique for Low Speed High Lift Airfoil Flowfield Analysis," *AGARD Conference Proceedings*, No. 291, Feb. 1981, pp. 26-1 to 26-10.

[5] Brune, G. W., Rubbert, P. E., and Nark, T. C. Jr., "A New Approach to Inviscid Flow/Boundary Layer Matching," AIAA Paper 74-601, June 1974.

[6] Catherall, D., Foster, D. N., and Sells, C.C.L., "Two Dimensional Incompressible Flow Past a Lifting Aerofoil," Royal Aircraft Establishment TR-69118, June 1969.

[7] Bristow, D. R., "Development of Panel Methods for Subsonic Analysis and Design," NASA CR-3234, Feb. 1980.

[8] Truckenbrodt, E., "A Method of Quadrature for Calculation of the Laminar and Turbulent Boundary Layer in Case of Plane and Rotationally Symmetrical Flow," NASA TM-1379, May 1955.

[9] McGhee, R. J. and Beasley, W. D., "Low Speed Aerodynamic Characteristics of a 17 Percent Thick Airfoil Section Designed for General Aviation Applications," NASA TN-D-7428, Dec. 1973.

[10] McGhee, R. J. and Beasley, W. D., "Low Speed Aerodynamic Characteristics of a 13-Percent-Thick Medium-Speed Airfoil Designed for General Aviation Applications," NASA TP-1498, Aug. 1979.